DETERMINATION OF PHYSICAL AND MECHANICAL PROPERTIES OF FINISHING PAPERS USED FOR WOOD-BASED COMPOSITE PRODUCTS

Anis Ben Amor
PhD Candidate

*Alain Cloutier**†
Professor

Robert Beauregard†
Professor
Centre de Recherche sur le Bois (CRB)
Département des Sciences du Bois et de la Forêt
Pavillon Gene-H.-Kruger
2425, rue de la Terrasse
Université Laval, Québec, QC, Canada, G1V 0A6

(Received October 2008)

Abstract. There has been a noticeable trend in the furniture and flooring industries in using finishing products (decorative paper, foil, wood veneer, and so on) of different quality on both surfaces of raw engineered wood-based panels. Under variable temperature and RH conditions, this practice can result in dimensional instability. The objective of this study was to determine the key properties of five finishing papers affecting the hygromechanical behavior of wood-based composite panels. The diffusion coefficients, swelling properties, and tensile modulus of elasticity (MOE) of the finishing papers were determined. The results show that the finishing papers studied are anisotropic in terms of their physicomechanical properties. For papers impregnated with melamine–formaldehyde resin, the tensile MOE decreases with an increase in resin content. Swelling is the most significant dimensional change. The range of variation of the linear expansion coefficients is between 0.03 and 0.17 in the fiber direction and between 0.08 and 0.28 in the transverse direction for raw papers. The linear contraction coefficients vary between 0.05 and 0.31 in the fiber direction and between 0.07 and 0.28 in the transverse direction. The behavior is different during adsorption and desorption. Effective diffusion coefficients of the papers tested vary between 4.5×10^{-12} and 8×10^{-11} m^2s^{-1}.

Keywords: Finishing papers, physicomechanical properties, engineered wood products, hygromechanical behavior.

INTRODUCTION

Adding value to wood-based composite panels through machining, finishing, and other processes involves knowledge of their detailed hygromechanical behavior in service. For economic and aesthetic reasons, a variety of finishing materials such as finishing papers, thermoplastic vinyl, veneer, and enamel are used for flooring, cabinet, and furniture products. Dimensional stability is of upmost importance in the use of raw wood-based composite panels in general and in finished ones in particular (NPA 1996). In the case of symmetrically coated wood-based composite panels exposed to RH variations, Jensen (2002) studied the influence of various finishing products, including veneer and enamel, on panel dimensional stability. For unbalanced finished panels subject to MC variations, warping leading to significant economic losses was observed (Suchsland and

* Corresponding author: Alain.Cloutier@sbf.ulaval.ca
† SWST member

McNatt 1985; Suchsland and Woodson 1986). The development of a model of the hygromechanical behavior of finished wood engineered products requires information about the wood-based panels (Ganev et al 2005a, 2005b), the adhesives (Wellons 1981; Baïlon and Dorlot 2000; Belleville 2008) and the finishing products. Little information on the diffusion and mechanical properties of finishing products, including resin-impregnated papers, is available. Harrisson (2005) obtained some data on the mechanical properties of finishing papers, but the number of paper types tested was limited.

Ganev (2002) established a 3-D model to characterize the hygromechanical behavior of raw medium-density fiberboard (MDF) panels. Blanchet et al (2006, 2007) developed the same type of model for unfinished and finished engineered wood flooring. The theoretical model proposed by Ganev (2005c) was based on three sets of equations: 1) 3-D equations of unsteady state moisture diffusion; 2) 3-D equations of mechanical equilibrium; and 3) Hooke's law taking into account the shrinkage and swelling of each layer through panel thickness. A sensitivity study of the model identified three dominant physicomechanical parameters controlling wood engineered material warping in the presence of MC gradients. Before modeling the hygromechanical behavior of finished wood products, three properties have to be identified for all components including the finishing papers: MOE, shrinkage, and expansion and diffusion coefficients. Wu and Suchsland (1996) determined the sorption curve and diffusion coefficient of high-pressure laminates (HPL) and HPL backer. The authors found that the diffusion coefficient increases with MC for both materials.

The objective of this work was to determine the physical and mechanical properties of finishing papers required to model the hygromechanical behavior of asymmetrically finished MDF, HDF, and particleboard products.

MATERIALS AND METHODS

Conditioning and Curing

Finishing papers impregnated with melamine-formaldehyde resin (MF) and caul plates were provided by Uniboard Canada Inc. Once received, the finishing papers were conditioned at 20°C and 60% RH. These papers are currently used in the manufacturing of laminate flooring and value-added wood-based panels for the furniture industry. Five different types of paper were considered: decorative papers DP162 and DP200, foil F40, backing layer BL220, and wear paper WP160. The physical characteristics of these finishing papers are given in Table 1.

Mechanical and physical tests were performed to determine the behavior of each paper as well as the compounded behavior of decorative and wear papers (DP162 + WP160). Papers DP162, DP200, WP160, DP162 + WP160, and BL220, impregnated with MF resin, were cured using a Becker & van Hüllen^{TM} press (600 × 600 mm) (Niederrheinische Maschinenfabrik GmbH, Kleve, Germany) at the Université Laval wood composites laboratory. Caul plates made of dolomite were used. The press platens temperature was 180°C and the pressure applied on the papers was 3.5 MPa. The pressing time was 20 s. The cured finishing papers were conditioned at 20°C and 60% RH for 2 wk before testing. The F40 paper was tested without being cured. Its industrial application on panel

Table 1. *Physical characteristics of the finishing papers.*

Paper type	Before resin impregnation (g/m^{-2})	After resin impregnation (g/m^{-2})	Resin content (based on OD mass; %)	Use
Decorative paper (DP162)	80	162	51	Flooring
Decorative paper (DP200)	80	200	60	Panels
Foil (F40)	40	40	0	Panels
Backing layer (BL220)	80	220	64	Flooring
Wear paper (WP160)	45	157	71	Flooring

surfaces requires a cold pressing process with polyvinylacetate and urea formaldehyde glue applied with dosing rollers. It was therefore impossible to isolate the finishing paper impregnated with the adhesive from the panel substrate. Moreover, information on the adhesive physicomechanical properties is available since several authors worked on UF resin properties (Wellons 1981; Dorlot et al 1986; Bodig and Jayne 1993) and later on PVA properties (Bandrup et al 1999; Baïlon and Dorlot 2000; Belleville et al 2008).

Determination of the Tensile Modulus of Elasticity

The tensile modulus of elasticity (MOE) of finishing papers was determined by adapting the TAPPI T 494 om-8 standard "Tensile properties of paper and paperboard (using a constant rate of elongation apparatus)" (TAPPI 1989). Two directions were considered in the paper plane: parallel and perpendicular to the principal fiber orientation to take into account the plane anisotropy of the material. For single-tested papers, a two-parameter (papers and directions) analysis of variance was performed using the SAS software (SAS Institute, Cary, NC). The 5% probability level was used. Ten test specimens per direction were cut from cured papers (DP162, BL220, WP160, and WP160 + DP162) and raw paper F40 with a laser cutter. The samples were 25 ± 1 mm wide with parallel edges within 0.1 mm and long enough to be clamped in the test machine rubber jaws with a test span of 180 ± 5 mm. The load was applied with a MTS universal testing machine model Q Test/5 (MTS Systems Corp, Eden Prairie, MN) at a rate of 25 ± 5 mm/min.

Determination of Expansion Properties

The expansion properties were determined as follows:

$$\mathrm{LE} = \frac{(\mathrm{L_{80}} - \mathrm{L_{50\_initial}}) \times 100}{\mathrm{L_{50\_initial}}} \quad (1)$$

$$\mathrm{LEC} = \frac{\mathrm{LE}}{\Delta\mathrm{MC}} \quad (2)$$

$$\mathrm{LC} = \frac{(\mathrm{L_{80}} - \mathrm{L_{50\ final}}) \times 100}{\mathrm{L_{80}}} \quad (3)$$

$$\mathrm{LCC} = \frac{\mathrm{LC}}{\Delta\mathrm{MC}} \quad (4)$$

$$\Delta\mathrm{MC} = \mathrm{MC_{80}} - \mathrm{MC_{50}} \quad (5)$$

where LE is the linear expansion (%); LEC is the linear expansion coefficient (dimensionless); LC is the linear contraction (%); LCC is the linear contraction coefficient (dimensionless); $L_{50\_initial}$ is the initial specimen length at equilibrium at 20°C and 50% RH (mm); L_{80} is the specimen length at equilibrium at 20°C and 80% RH (mm); L_{50_final} is the final specimen length after reconditioning to 20°C and 50% RH (mm); $\triangle$MC is the MC increase or decrease (%); MC_{80} is the MC at 80% RH (%); and MC_{50} is the MC at 50% RH (%).

The change in length was monitored at 20°C from 50–80% RH in adsorption and then from 80–50% RH in desorption on the same specimens and measured with a caliper. The RH conditions were obtained using a climate chamber, model SH27 (Envirotronics, Grand Rapids, MI). Ten specimens were tested per direction in the paper plane. At each equilibrium level, the length and mass of the specimens were recorded. At the end of the test, paper specimens were oven-dried, and MC at each RH level was determined according to ASTM D 1037-99.

Determination of Swelling Properties

To evaluate thickness swelling (TS), 10 LE specimens per direction in the paper plane were used. The specimen thickness at three points midway across the specimen width was measured with a micrometer. The thicknesses were noted once equilibrium was reached at

50 and 80% RH and after reconditioning to 50% RH. The swelling properties were determined as follows:

$$TS = \frac{(T_{80} - T_{50\ initial}) \times 100}{T_{50\ initial}} \quad (6)$$

$$TSC = \frac{TS}{\Delta MC} \quad (7)$$

$$TSh = \frac{(T_{80} - T_{50\ final}) \times 100}{T_{80}} \quad (8)$$

$$TShC = \frac{TSh}{\Delta MC} \quad (9)$$

where TS is the thickness swell as percent; TSC is the thickness swell coefficient, (dimensionless); TSh is the thickness shrinkage as percent; TShC is the thickness shrinkage coefficient (dimensionless); $T_{50\_initial}$ is the initial specimen thickness after conditioning to 50% RH before exposure at 80% RH; T_{80} is the specimen thickness at equilibrium at 80% RH; and $T_{50\ final}$ is the final specimen thickness after reconditioning to 50% RH.

Determination of Diffusion Coefficient

The moisture diffusion coefficient (D) of finishing papers was determined by adapting the vapor cup method (Siau 1995). Empty glass pots were used as vapor cups (Fig 1). They were cleaned with acetone and two Teflon seals were applied along the contour of the pot. The pot lid was perforated with a 40-mm-dia hole. It was then sanded with an abrasive paper to ensure better adhesion between the metal lid and the finishing product (Fig 2a). On the top of the lid, a finishing paper was glued with 5-min epoxy (Lepage, Henkel Canada Corp, Mississauga, Canada). Distilled water (100 mL) was added to the vapor cup. The lid was tightened and the vapor cup was placed in a conditioning chamber at 20°C and 50% RH (Fig 2b).

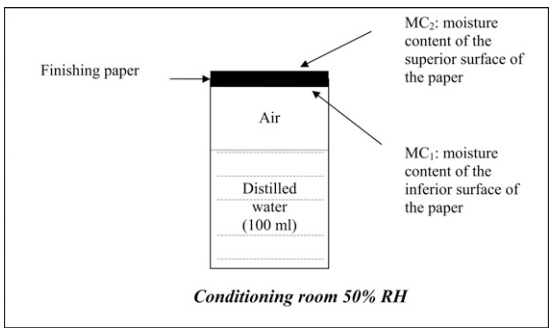

Figure 1. Vapor cup assembly in conditioning room (adapted from Siau (1995)).

The moisture diffusion coefficient (D) was determined as follows:

$$D = \frac{100 \times \Delta w \times l}{\Delta t \times A \times \rho_w \times G \times \Delta MC} \quad (10)$$

where Δw is the mass variation of the vapor cup in kilograms; l is thickness of the finishing paper in meters; Δt is the time interval in seconds; A is the surface of diffusion contact (circle), m^2; ρ_w is the density of water, 1000 kg/m^{-3}; G is the specific gravity of the finishing paper; $\Delta MC = MC_2 - MC_1$; MC_1 is the MC of the finishing paper surface inside the cell at 90% RH; and MC_2 is the MC of the finishing paper surface outside the cell at 50% RH.

Five specimens of each paper type were conditioned at 50 and 90% RH in a climate chamber, model SH27 from Envirotronics®. At the end of the test, the specimens were oven-dried. Therefore, G and MC at each level of RH (conditioning chamber and inside the cell) were determined according to ASTM D 1037-99 (MC and specific gravity), and used to determine ΔMC in Eq 10.

The cell mass (w) was measured throughout the diffusion process. The curve of the vapor cup mass as a function of time (t) shows two phases: curvilinear and linear. The slope of the linear part of the vapor cup mass against time curve $(\frac{\Delta w}{\Delta t})$ was used in the calculation of D for steady-state moisture diffusion.

(a) (b)

Figure 2. (a) Perforated vapor cup lid; (b) vapor cup assembly.

RESULTS AND DISCUSSION

Tensile Modulus of Elasticity

The results obtained for the tensile MOE of the finishing papers studied are presented in Table 2 for single-cured papers (DP162, DP200, WP160, and BL220), the composite papers α and β (WP160 + DP162), and raw paper F40. For single-tested papers, a two-parameter analysis of variance (paper type and direction) was performed with SAS software. The analysis of variance presented in Table 3 shows highly significant effects and interaction of paper type and direction.

To understand the interaction between paper type and direction, a Duncan multiple comparisons test was performed. The results show that for a given single-tested paper, the tensile MOE in the direction of fiber orientation (MOE_1) is higher than that in the transverse direction (MOE_2) for DP162, DP200, F40, BL220, and WP160. These finishing papers are orthotropic, which involves different physical and mechanical properties according to the three principal directions considered.

There was a significant variation in tensile MOE between single-cured papers. We found the following MOE_1 for the press-cured finishing papers in descending order: 7.92 GPa for DP162, 6.48 GPa for DP200, 5.71 GPa for the backing layer BL220, and finally 4.76 GPa for the wear paper WP160. The MOE in the transverse direction MOE_2 shows the same trend. We found in descending order: 6.68 GPa for DP162, 5.49 GPa for DP200, 5.09 for the backing layer BL220, and finally 3.83 for the wear paper WP160.

The relation between resin content and MOE was studied for single-cured papers. The contrast analysis presented in Table 4 shows that MOE and resin content vary conversely. These results are in agreement with those obtained by Harrisson (2005), which showed that the tensile MOE linearly decreased with an increase in resin content. It is important to notice that the MOE values obtained in the current study are smaller than those obtained by Harrisson (2005) for similar papers. The MOE values measured in the two principal plane directions by Harrisson (2005) are 15% higher for DP162 and BL220 and 20% higher for WP160. Variability of the finishing paper properties between both studies most likely explains the differences. The raw finishing paper F40 shows the lowest tensile MOE (4.01 GPa) in the fiber direction and (2.75 GPa) in the transverse direction.

Table 2. *Summary of the results obtained for tensile modulus of elasticity, diffusion, linear expansion, linear contraction, thickness swelling and thickness shrinkage coefficients for the papers tested.*

	MOE_1		MOE_2		D		LEC_1		LEC_2		LCC_1		LCC_2		TSC		TShC	
Paper type	Mean (GPa)	Duncan grouping	Mean (GPa)	Duncan grouping	Mean (m^2s^{-1})	Duncan grouping	Mean (%/%)	Duncan grouping	Mean (%/%)	Duncan grouping	Mean (%/%)	Duncan grouping	Mean (%/%)	Duncan grouping	Mean (%/%)	Duncan grouping	Mean (%/%)	Duncan grouping
DP162	7.92	A	6.68	A	4.55×10^{-12}	D	0.17	B	0.26	A	0.14	B	0.23	C	1.39	B	0.88	DE
	(0.46)		(0.19)		(4×10^{-13})		(0.05)		(0.04)		(0.02)		(0.03)		(0.30)		(0.04)	
DP200	6.48	B	5.49	B	4.79×10^{-12}	D	0.14	CB	0.28	A	0.05	D	0.28	A	1.51	B	0.78	E
	(0.39)		(0.37)		(3×10^{-13})		(0.02)		(0.02)		(0.01)		(0.02)		(0.25)		(0.10)	
WP160	4.76	D	3.83	D	8.11×10^{-11}	A	0.09	D	0.18	C	0.06	D	0.18	D	1.26	B	0.98	CD
	(0.65)		(0.34)		(6.6×10^{-12})		(0.02)		(0.03)		(0.01)		(0.03)		(0.05)		(0.18)	
BL220	5.71	C	5.09	C	9.74×10^{-12}	C	0.11	CD	0.22	B	0.17	C	0.18	D	1.45	B	1.07	BC
	(0.23)		(0.37)		(1×10^{-12})		(0.02)		(0.05)		(0.05)		(0.03)		(0.22)		(0.13)	
α	4.75	D	3.25	E	1.7×10^{-11}	B	0.15	CB	0.24	A	0.15	B	0.25	B	2.72	A	1.13	AB
	(0.41)		(0.43)		(8×10^{-13})		(0.02)		(0.05)		(0.02)		(0.03)		(0.37)		(0.17)	
β	4.00	E	3.63	D	1.8×10^{-11}	B	0.26	A	0.17	C	0.31	A	0.18	D	2.82	A	1.25	A
	(0.42)		(0.09)		(1×10^{-12})		(0.08)		(0.04)		(0.06)		(0.03)		(0.06)		(0.41)	
F40	4.01	E	2.75	F	9.48×10^{-12}	C	0.03	E	0.08	D	0.07	D	0.07	E	0.55	C	0.50	F
	(0.17)		(0.28)		(4×10^{-13})		(0.01)		(0.01)		(0.01)		(0.01)		(0.08)		(0.08)	

Standard deviation in parentheses. Means with different letters are significantly different ($p \leq 0.05$).

α: WP160 + DP162 with fiber direction parallel.

β: WP160 + DP162 with fiber direction perpendicular.

To quantify paper anisotropy, we can define γ as follows:

$$\gamma = \frac{(MOE_1 - MOE_2) \times 100}{MOE_2} \qquad (11)$$

Table 5 shows γ values for all tested papers and compares them with those obtained by Harrisson (2005). The γ values obtained in the current study are smaller than those obtained by Harrisson (2005) for DP162 (18.5% compared with 25.0%) and WP160 (24.0% compared with 30.3%). The same level of anisotropy was found for BL220 (γ of about 12.0% in both cases). With a γ value of 45.6%, the raw paper F40 is highly anisotropic.

Because each component is an orthotropic material, the WP160 + DP162 composite paper depends on the orientation of each paper component. Two paper orientations were considered: α (WP160 + DP162) where the fiber direction of both papers was parallel and β (WP160 + DP162) where the fiber direction of both papers was perpendicular.

By convention, the fiber direction of the composite paper (WP160 + DP162) is the fiber direction of WP160. As shown in Table 5, the β-combination results in a quasi-isotropic material (γ = 10.3%), whereas the α-combination is highly anisotropic (γ = 46.4%). It seems that the orientation of WP160 in the composite paper WP160 + DP162 controls its MOE in tension. The Duncan test shows no significant differences between the mean MOE_1 obtained for WP160 and the α-combination and between the mean MOE_2 obtained for WP160 and the β-combination (Table 2).

Table 3. *Analysis of variance for tensile modulus of elasticity of single-cured papers.*

Effect	Degree of freedom	F value
Paper type	4	299.56***
Fiber direction	1	41.27***
Paper type*fiber direction	4	33.10***

*** Significant with a probability level > 99%.

Table 4. *Contrast analysis test for single cured papers: effect of resin content.*

	Estimated gradient of MOE	Standard error	t value	Probability
Resin content	–149.92	9.82	–15.26	<0.0001

Expansion Coefficients

Table 2 shows the results obtained for the linear expansion, linear contraction, and thickness swelling coefficients. A Duncan's multiple range test on the mean LEC, LCC, TSC, and TShC obtained as a function of paper type is also presented.

For each finishing paper, TSC is the highest with values in the order of 1%/% MC change. The higher TSC was obtained for paper DP200 at 1.51%/% MC. This is more than five times the LEC in the transverse direction (0.28) and nearly 11 times the LEC in the fiber direction (0.14). The same trend is observed for all tested papers with different proportions between TSC and LEC.

For each single-tested paper (DP200, DP162, WP160, BL220, and F40) in adsorption, LEC

Table 5. *Degree of anisotropy (γ) in finishing papers compared with the literature.*

Paper type	γ (%)	γ (Harrisson 2005) (%)
Press cured papers		
DP162	18.5	25
DP200	18	xxx
WP160	24	30.25
BL220	12.3	11.82
DP162 + WP160$^{(\alpha)}$	46.4	xxx
DP162 + WP160$^{(\beta)}$	10.3	xxx
Raw paper		
F40	45.6	xxx

Table 6. *Results of analysis of variance for the impact of the paper type and fiber direction on the LEC.*

Effect	Degree of freedom	F value
Paper type	6	54.89***
Fiber direction	1	122.61***
Paper type* fiber direction	6	23.24***

*** Significant with a probability level > 99%.

in the transverse direction (0.28, 0.26, 0.18, 0.22, and 0.08, respectively) is nearly twice as much as those in the fiber direction (0.14, 0.17, 0.09, 0.11, and 0.03, respectively). These results confirm the anisotropy of these materials. The analysis of variance was performed by comparing the LEC obtained for the different paper types (Table 6). The F-values show highly significant effects of paper type and fiber direction. Moreover, a highly significant interaction between paper and fiber direction was found. It is worth mentioning that the behavior of the papers is different during adsorption and desorption. Wu and Suchsland (1996) also found sorption hysteresis when they tested HPL and HPL backer. The TSC obtained for DP200, DP162, WP160, BL220, α, β, and F40 confirm this point. They were 1.51, 1.39, 1.26, 1.45, 2.72, 2.82, and 0.55, respectively, compared with TShC of 0.78, 0.88, 0.98, 1.07, 1.13, 1.25, and 0.50.

The orientation of DP162 in the composite paper (WP160 + DP162) controls its expansion properties. The LEC obtained for DP162 are 0.17 in the fiber direction and 0.26 in the transverse direction. In the case of the α-combination in which both fiber orientations are parallel, the expansion properties of the whole material follow the trend of DP162. The LECs for the α-combination are 0.15 and 0.24 in the fiber direction and transverse direction, respectively. In the case of the β-combination, the expansion properties are inverted (LEC of 0.26 in the fiber direction and 0.17 in the transverse direction) compared with the α-combination in which the fiber direction of paper DP162 corresponds to the transverse direction of the composite paper.

Effective Diffusion Coefficient

The vapor cup test was performed for each finishing paper. Figure 3 shows the average mass of the vapor cup against time. For each material studied, the curve shows two moisture diffusion phases: a nonlinear unsteady state at the start of the process and a linear steady state until the end.

Decorative paper (DP200 and DP162) vapor cups lost less water than the other papers. For the same paper quality, it seems that resin content and mass loss rate vary conversely ($\frac{\Delta w}{\Delta t}$ = –0.0016 g/h for DP200 and –0.0041 g/h for DP162). The second diffusion group includes three finishing products: α, BL220, and β.

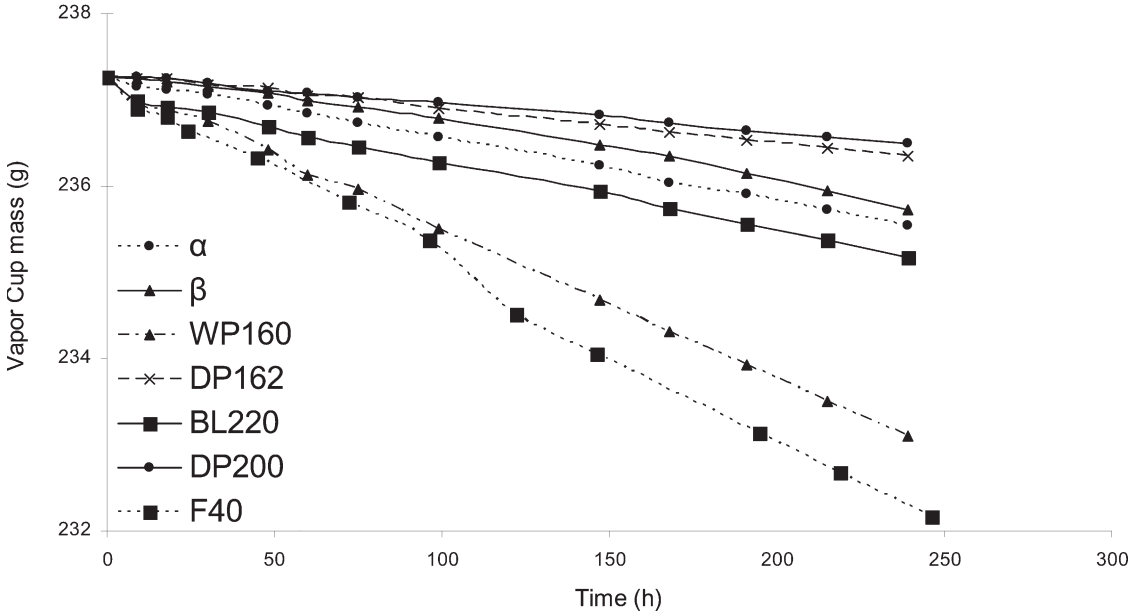

Figure 3. Vapor cup mass (g) as a function of time (h) for the finishing papers.

The cell mass loss rates ($\frac{\Delta w}{\Delta t}$) are, respectively: –0.0075, –0.0081, and –0.0085 g/h. Finally, we found that F40 and WP160 show the two highest mass loss rates calculated in the steady state. For foil paper F40, the low density and thickness, and the absence of adhesive acting as a barrier against moisture explain the results.

Table 2 shows the average diffusion coefficients obtained for the seven finishing papers. The analysis of variance shows highly significant effects of paper type on the measured diffusion coefficients (Table 2). The introduction of WP160 into flooring products aims to protect decorative paper from abrasion and scratches. However, this material shows the highest effective diffusion coefficient, which can affect engineered wood flooring dimensional stability. It is important to notice that WP160 has a resin content of 71%. The high value of D for this material can be explained by the low value of $|\Delta MC| = 0.9$ compared with the other papers: $|\Delta MC| = 2.5$ for DP162, 2.5 for the α-combination and 3.1 for BL220; and by the low value of $G = 0.73$ compared with the other papers: $G = 1.0$ for the α- and β-combinations and 1.05 for DP200. Other aspects can also influence D such as fiber morphology, manufacturing process, and- resin distribution. The decorative paper DP162 shows the lower diffusion coefficient. When cured with WP160, both composite papers (α and β) have diffusion coefficients between those of DP162 and WP160.

These results can be applied to industrial applications. We can consider the case of a raw MDF panel finished asymmetrically with F40 on one face and DP200 on the other. In the case of a change in ambient RH, moisture diffusion from both surfaces will be nonuniform because the measured diffusion coefficients are 9.48×10^{-12} m^2s^{-1} for foil and 4.79×10^{-12} m^2s^{-1} for decorative paper. This practice results in a MC gradient across panel thickness and induces stress in the panel causing deformations and a reduced product value. The industrial case of laminate flooring (α- or β-combination and BL220) shows nearly the same situation. The diffusion coefficient of the top surface (α or β) is twice as much as the bottom one BL220, which should result in an asymmetrical and unbalanced diffusion behavior. A numerical model of moisture diffusion and mechanical behavior of finished wood-based composite panels should be developed using the material characteristics determined in this paper. Such a model would be useful in the development of future products finished with unbalanced papers.

CONCLUSIONS

Physical and mechanical properties of finishing papers used for wood engineered products were determined. The following results were obtained.

Finishing papers are anisotropic with regard to their physical and mechanical properties. Two principal directions must be considered in the paper plane: fiber and transverse. The tensile MOE measured in the fiber direction was between 18 and 45.6% higher than in the transverse direction for single finishing papers.

For papers impregnated with melamine formaldehyde resin, the MOE decreased with resin content. The resin content varies from 51% for paper DP162 to 71% for paper WP160. The corresponding decrease in MOE between these two papers is 39.9% in the fiber direction and 42.7% in the transverse.

The cured combination of decorative paper and wear paper was studied. When the fiber direction of each paper is perpendicular, the resulting material shows a more isotropic behavior.

For all tested papers (DP162, DP200, WP160, BL220, α, β, and F40), the linear expansion and linear contraction coefficients during adsorption and desorption were different.

In the presence of a MC change, thickness swelling and shrinkage are the most important dimensional changes.

The orientation of paper DP162 controls the linear expansion and contraction coefficients of the composite paper made from WP160 and DP162. However, the orientation of paper WP160 controls MOE in tension.

ACKNOWLEDGMENTS

We are grateful to NSERC and the industry partners of CIBISA "Chaire Industrielle sur les bois d'Ingénierie Structuraux et d'Apparence" for financing the project and to Uniboard Canada Inc. for providing the finishing papers and caul plates. We also thank Les Industries de la Rive Sud for their collaboration and Mr. David Lagueux for technical assistance.

REFERENCES

Baïlon J-P, Dorlot J-M (2000) Des Matériaux. [Materials (in French).] 3rd ed. École Polytechnique de Montreal. 740 pp.

Bandrup I, Immergut EH, Grulke EA (1999) Polymer handbook. 4th ed. John Wiley & Sons, New York, NY. 2288 pp.

Belleville B, Cloutier A, Blanchet P (2008) Wood-adhesive interface characterization and modeling in engineered wood flooring. Wood Fiber Sci 40(4): 484 – 494.

Blanchet P, Cloutier A, Gendron G, Beauregard R (2006) Engineered wood flooring design using the finite element method. Forest Prod J 56(5):59 – 65.

——— (2007) Numerical prediction of engineered wood flooring deformation. Wood Fiber Sci 37(3):484 – 496.

Bodig J, Jayne BA (1993) Mechanics of wood composites. Krieger Publishing Company, Malabor, FL. 712 pp.

Dorlot J-M, Baïlon J-P, Masounave J (1986) Des matériaux. École Polytechnique de Montréal, Québec. 467 pp.

Ganev S (2002) Modeling of the hygro-mechanical warping of medium density fiberboard. Doctoral thesis, Département des Sciences du Bois, Université Laval, Québec, QC, Canada. 157 pp.

———, Cloutier A, Gendron G, Beauregard R (2005a) Mechanical properties of MDF as a function of density and moisture content. Wood Fiber Sci 37(2): 314 – 326.

——— (2005b) Linear expansion and thickness swell of MDF as a function of panel density and sorption state. Wood Fiber Sci 37(2):327 – 336.

——— (2005c) Finite elements modeling of the hygroscopic warping of medium density fiberboard. Wood Fiber Sci 37(2):337 – 354.

Harrisson L (2005) Caractérisation des papiers de finition et des panneaux de fibres de bois de haute densité (HDF) utilises dans la production de plancher flottant. [Characterization of the finishing papers and of the high density fiberboards (HDF) used for floating parquet flooring (in French).] Master thesis, Université Laval, Québec, QC, Canada. 95 pp.

Jensen U (2002) Asymmetric coating of 3D fronts a risk for dimensional stability? Conference in Institüt für Holztechnologie, Dresden, Germany. 11 pp.

NPA (1996) Standard method for measuring of warp in particleboard and medium density fiberboard (MDF). National Particleboard Association NPA18928. Premiere Court, Gaithersburg, MD.

Siau JF (1995) Wood: Influence of moisture on physical properties. Department of Wood Science and Forest Products, Virginia Polytechnic Institute and State University. 227 pp.

Suchsland O, McNatt JD (1985) On the warping of laminated wood panels. Michigan State University, East Lansing, MI. 120 pp.

———, Woodson GE (1986) Fiberboard manufacturing practises in the United States. USDA Forest Service. Agri. Handbook No. 640. 263 pp.

TAPPI (1989) TAPPI test methods. Vol. 1. T 494 om-88. Tensile breaking properties of paper and paperboard (using constant rate of elongation apparatus). Technical Association for the Worldwide Pulp, Paper, and Converting Industry, Atlanta, GA.

Wellons JD (1981) The adherents and their preparation for bonding. Pages 87 – 134 *in* Adhesive bonding of wood and other structural materials. Forest Products Laboratory, Forest Service, USDA and University of Wisconsin. A publication of the Educational Modules for Materials Science and Engineering (EMMSE) Project. Material Research Laboratory, The Pennsylvania State University, State College, PA.

Wu Q, Suchsland O (1996) Prediction of moisture content and moisture gradient of an overlaid particleboard. Wood Fiber Sci 28(2):227 – 239.